# We are IntechOpen, the world's leading publisher of Open Access books Built by scientists, for scientists

**4,800**
Open access books available

**122,000**
International authors and editors

**135M**
Downloads

Our authors are among the

**154**
Countries delivered to

**TOP 1%**
most cited scientists

**12.2%**
Contributors from top 500 universities

CLARIVATE ANALYTICS BOOK CITATION INDEX INDEXED

WEB OF SCIENCE™

Selection of our books indexed in the Book Citation Index in Web of Science™ Core Collection (BKCI)

## Interested in publishing with us?
## Contact book.department@intechopen.com

Numbers displayed above are based on latest data collected.
For more information visit www.intechopen.com

Chapter 5

# Second Harmonic Generation Microscopy: A Tool for Quantitative Analysis of Tissues

Juan M. Bueno, Francisco J. Ávila, and Pablo Artal

Additional information is available at the end of the chapter

http://dx.doi.org/10.5772/63493

## Abstract

Second harmonic generation (SHG) is a second-order non-linear optical process produced in birefringent crystals or in biological tissues with non-centrosymmetric structure such as collagen or microtubules structures. SHG signal originates from two excitation photons which interact with the material and are "reconverted" to form a new emitted photon with half of wavelength. Although theoretically predicted by Maria Göpert-Mayer in 1930s, the experimental SHG demonstration arrived with the invention of the laser in the 1960s. SHG was first obtained in ruby by using a high excitation oscillator. After that starting point, the harmonic generation reached an increasing interest and importance, based on its applications to characterize biological tissues using multiphoton microscopes. In particular, collagen has been one of the most often analyzed structures since it provides an efficient SHG signal. In late 1970s, it was discovered that SHG signal took place in three-dimensional optical interaction at the focal point of a microscope objective with high numerical aperture. This finding allowed researchers to develop microscopes with 3D submicron resolution and an in depth analysis of biological specimens. Since SHG is a polarization-sensitive non-linear optical process, the implementation of polarization into multiphoton microscopes has allowed the study of both molecular architecture and fibrilar distribution of type-I collagen fibers. The analysis of collagen-based structures is particularly interesting since they represent 80% of the connective tissue of the human body. On the other hand, more recent techniques such as pulse compression of laser pulses or adaptive optics have been applied to SHG microscopy in order to improve the visualization of features. The combination of these techniques permit the reduction of the laser power required to produce efficient SHG signal and therefore photo-toxicity and photo-damage are avoided (critical parameters in biomedical applications). Some pathologies such as cancer or fibrosis are related to collagen disorders. These are thought to appear at molecular scale before the micrometric structure is affected. In this sense, SHG imaging has emerged as a powerful tool in biomedicine and it might serve as a non-invasive early diagnosis technique.

**Keywords:** second harmonic microscopy, biomedical imaging, collagen, polarization, adaptive optics

## 1. Principles of second harmonic generation

Non-linear optical microscopy refers to all microscopy techniques based on non-linear optics, in which light-matter interactions violate the linear superposition principle. These techniques can be divided in two main categories: incoherent and coherent. Although in the former, the phase of the emitted optical signal is random, in coherent techniques it depends on a wide variety of factors, including those related to the exciting light or associated with the geometric distribution of the radiating molecules. One of these phenomena is the so called Second Harmonic Generation (SHG).

SHG is a coherent non-linear process where two incident photons at their fundamental frequency interacting with a medium are directly converted into a single photon of exactly the same total energy at double of frequency, without absorption or reemission of photons [1]. This process is carried out via an intermediate virtual state in a single quantum event. **Figure 1** compares this SHG process with the typical linear fluorescence phenomenon.

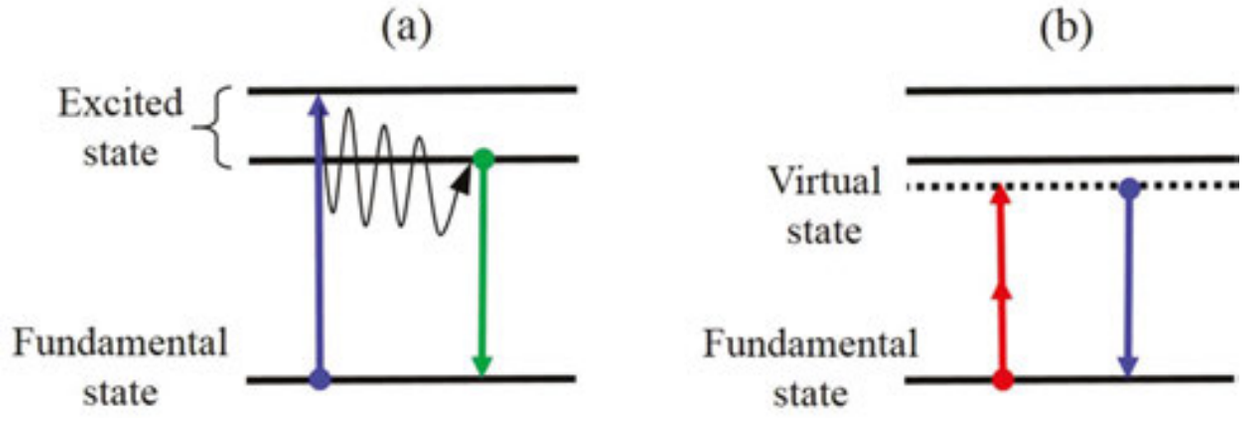


**Figure 1.** Diagrams of linear fluorescence (a) and SHG (b).

According to the non-linear optics theory, an incident electric field $\vec{E}_{\omega}$ with a frequency $\omega$ induces a second-order polarization $\vec{P}_{2\omega,i}$ at $2\omega$ in the $i$th direction given by [1]:

$$\vec{P}_{2\omega,i} = \varepsilon_0[\chi^{(1)}\vec{E} + \chi^{(2)}\vec{E}\vec{E} + \chi^{(3)}\vec{E}\vec{E}\vec{E} + ...] \quad (1)$$

http://dx.doi.org/10.5772/63493

where $\varepsilon_0$ is the vacuum permittivity and $\chi^{(n)}$ is the $n$th-order non-linear susceptibility tensor. The first term of Equation (1) describes the normal absorption and reflection of light, and the second the SHG. Since the term $\chi^{(2)}$ depends on the polarization of the excitation source, the SHG emission is sensitive to polarization [2]. In a medium with hexagonal symmetry, the non-null coefficients $d_{ij} = \frac{1}{2}\varepsilon_0 \chi_{ij}^{(2)}$ are $d_{31}$, $d_{33}$, $d_{15}$ and $d_{14}$ [3].

These coefficients contain the non-linear optical properties of the material and sum zero for inversion symmetry [4]. Moreover, if Kleinman and cylindrical symmetries are assumed, $d_{14}$=0 and $d_{15} = d_{31}$ [5].

SHG was demonstrated in crystalline quartz in 1962 by Kleinman, and since then this has been commonly used to frequency-double pulsed lasers to obtain shorter wavelengths [5]. Moreover, SHG signal is sensitive to bulk non-centrosymmetric spatial arrangements such as collagen structures or birefringent crystals [6]. The lack of a center of symmetry in an organized material strongly affects the second-order susceptibility and therefore the efficiency of SHG signals [7].

Unlike two-photon excitation fluorescence, SHG is energy conserving (it does not involve an excited state), strongly directional and preserves the coherence of the laser light [8]. Then, a medium is able to provide efficient SHG signal when its structure is organized at the scale of the laser wavelength and lacks a center of symmetry. Further details on the advantages of using SHG imaging (especially for biological applications) will be presented along this chapter.

## 2. SHG microscopy of biological samples

In 1971, Fine and Hansen proposed that SHG signal could also be produced by biological tissues [9]. In 1974, Hellwarth and Christensen implemented SHG into an optical microscope to visualize the microscopic crystal structure of polycrystalline ZnSe [10]. Later, Gannaway and Sheppard presented SHG images of a lithium niobate crystal by using a laser scanning microscope [11]. These images showed features and contrast levels not seen in regular (linear) microscopy.

However, to our knowledge, the first biological SHG image was reported by Freund in 1986. He imaged a rat tail tendon with high resolution SHG scanning microscopy [12]. More than a decade was necessary to consistently apply SHG microscopy to visualize biological specimens. In particular, a laser scanning microscope was combined with a Ti-Saphire femtosecond laser to acquire live cell images based on SHG [13].

Other biological specimens imaged using SHG microscopy include membranes [7], proteins [13] and collagen-based structures [14] among others. **Figure 2** shows a sample containing starch grains imaged with SHG microscopy.

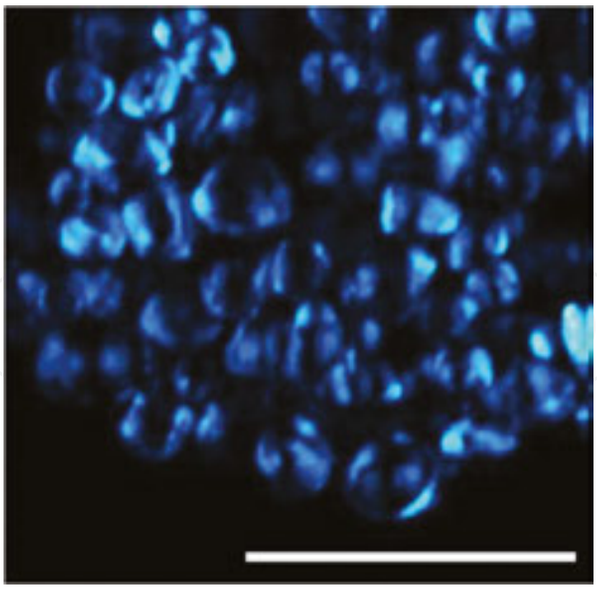

**Figure 2.** SHG image of starch grains. These are plant polysaccharides with a convenient radial structure. It can be found in both a non-organized (dry) and an organized (hydrated) form. Scale bar: 50 μm.

According to the non-linear nature of harmonic generation, the intensity of the SHG signal depends on the square of the excitation laser intensity, and occurs intrinsically confining the focus of the microscope objective. Since this event takes place in both transversal and axial directions, SHG imaging microscopy provides intrinsic 3D sectioning capabilities with excellent Z-resolution. This property allows optical sectioning of biological samples with reduced out-of-plane photo-toxicity (see **Figure 3**).

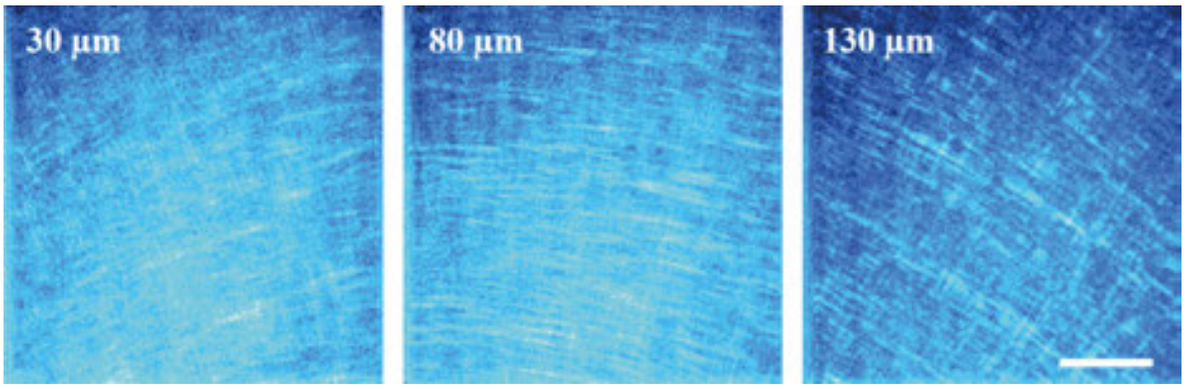


**Figure 3.** SHG images of an eagle cornea acquired at three different depth locations. Scale bar: 50 μm.

Apart from this inherent property, during the last ten years SHG microscopy has gained increasing popularity in biomedicine mainly due to the provided possibilities for endogenous contrast imaging (staining procedures are not required), reduced tissue damage, sensitivity to molecular architecture organization, preservation of phase information and polarization dependence [15].

http://dx.doi.org/10.5772/63493

SHG is restricted to molecules with non-centrosymmetric organization and is emitted by different biological tissues containing collagen [1], myosin [16] or tubulin (which polymerizes into microtubules) [17]. Type-I collagen is the most abundant structural protein of the human body [18], and due to its presence in connective tissue, SHG signal can be effectively obtained from the cornea, the skin, bones or tendons [19–27]. Collagen plays an important role within the human body and has been studied under many different experimental conditions. Its presence in connective tissues constitutes 6% of the dry weight of the body [28].

The basic structural unit of collagen is the molecule of tropocollagen, presenting a helical structure, formed by three polypeptide chains coiled around each other to form a spiral (see **Figure 4**). These molecules are cross-linked to form collagen fibrils.

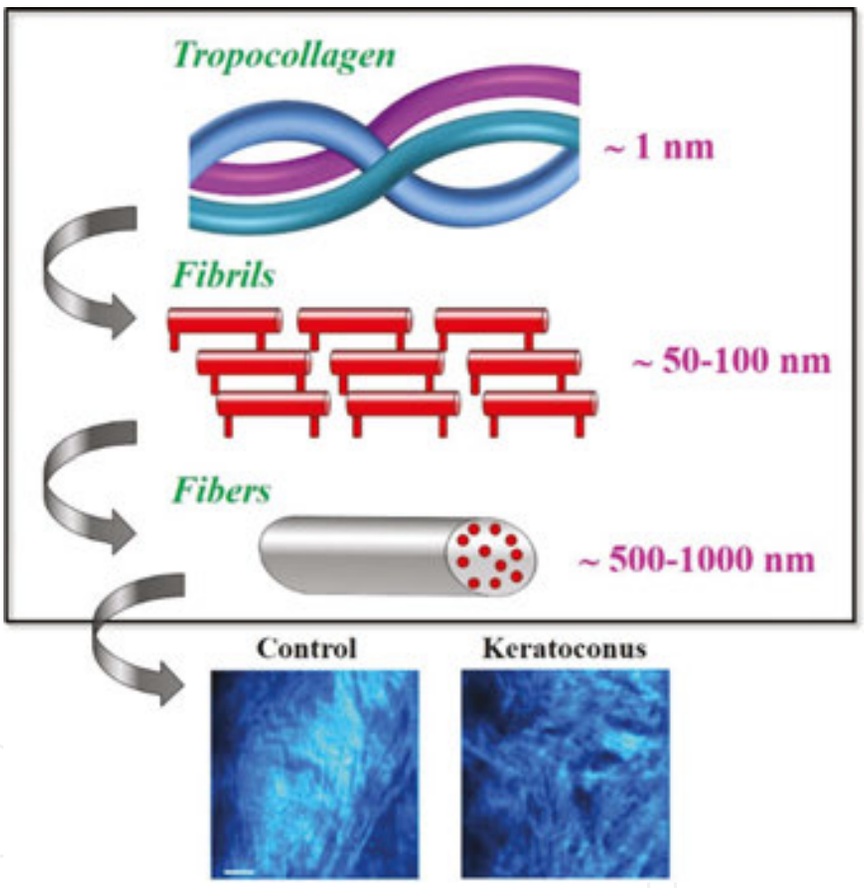


**Figure 4.** Schematic representation of the collagen structure and SHG images of two human corneas with different collagen distributions. Bar length: 50 μm.

These fibrils are assembled into parallel beams to form collagen fibers [18]. The origin of the SHG signal in collagen arises from its molecular chirality, where the molecules possess permanent dipole moments with high order alignment, ensuring the generation of harmonic signal as a consequence of the non-symmetrical oscillation of the electrons [15]. On the other hand, the intrinsic chirality of the triple-helix of molecular collagen increases the asymmetry of the assembly increasing the non-linear response.

As above explained, the SHG signal can be characterized by the non-linear susceptibility tensor [4]. This depends on the induced dipole moment of the molecules and therefore on the organization of the collagen tissue. If a collagen triple-helix is excited along its main axis, each bond contribution is summed coherently to the SHG signal [29]. When the molecules with the same orientation—or polarity—are assembled to form fibrils, the SHG signal is amplified significantly [30]. Then, the total intensity is the coherent sum of the signal from individual collagen fibrils.

However, in some collagen-based tissues the polarity of the fibrils within the fiber varies randomly [31]. In those cases the organization presents contributions to the axial momentum altering the coherent process of the SHG. Theoretically, the phase matching condition for which the non-linear process is strictly coherent is given by [15]:

$$\overrightarrow{\Delta k} = \overrightarrow{k_{2\omega}} - \overrightarrow{2k_{\omega}} = 0 \tag{2}$$

where $\overrightarrow{k_{2\omega}}$ is the wave vector for the SHG emission and $\overrightarrow{2k_{\omega}}$ is the wave vector of the incident light. Then, a second harmonic conversion is maximum if $\Delta\vec{k}=0$. Experimentally, only birefringent crystals have been found to verify this condition [32]. In biological samples, and particularly in collagen-based tissues, the SHG signal is a quasi-coherent process which SHG efficiency conversion depends on how aligned within the fiber the fibrils are.

SHG images at the bottom of **Figure 4** compare the collagen distribution in a normal healthy human cornea and another affected by a pathology called keratoconus. This is a real example on how the coherence of SHG signal is an efficient detector of collagen organization within a sample. Although the control tissue displays a fairly regular distribution of collagen fibers along a preferential direction, these are randomly distributed in the pathologic case. The

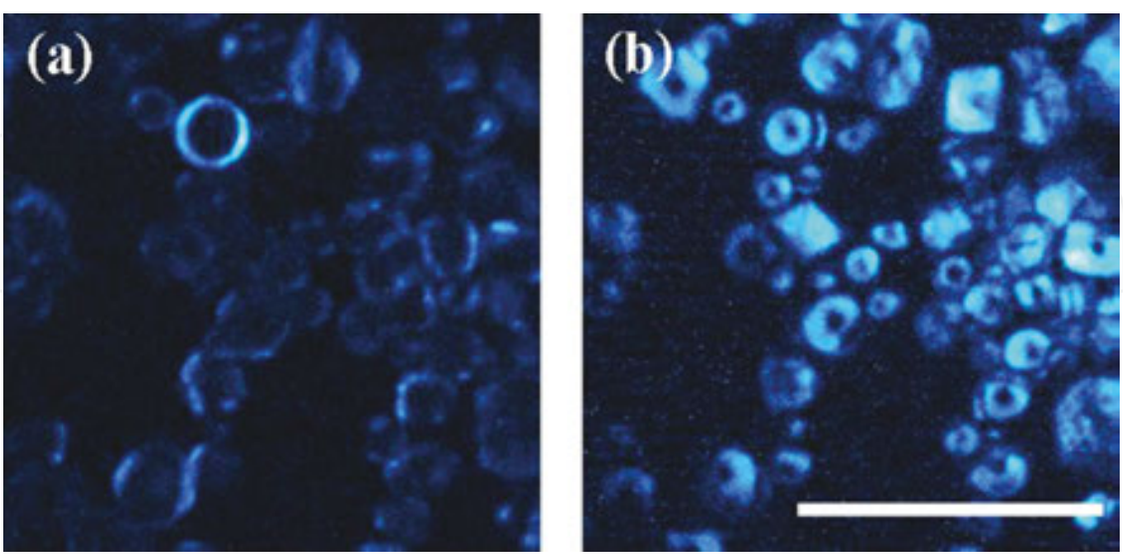


**Figure 5.** Comparison of SHG images acquired in the backward (a) and forward (b) directions. The differences between the two acquisition directions are readily visible due to the behavior of the SHG emission. Scale bar: 50 μm.

control tissue provides a more efficient SHG conversion because $\Delta\vec{k}$ is significantly lower than in the pathologic case. Changes in collagen morphology are firstly produced at molecular level (tropocollagen), which number of aligned dipoles coherently sum, affecting the fibril organization and therefore the distribution of the fibers finally imaged with SHG microscopy.

On the other hand, the emission directionality has an effect in both SHG signal conversion efficiency and observed morphology. This is easy observed in the starch grains presented in **Figure 5**.

In collagen-based tissues, this effect is due to the size and the organization of the collagen fibers, since both affect the phase mismatch and the amplification of the SHG intensity [15]. In general, SHG directionality depends on the distribution of the induced dipoles in the focal volume where the non-linear process takes place [33]. In this sense, the directionality effects of the SHG signal can be appreciated in the visualization of continuous structures (fibers) in the backward channel (i.e. backscattered emission), and a higher segmentation or discrete distribution in the forward directed emission [34]. This implies that the choice of the detection direction in the experimental device will depend on the desired scale of observation. However, since changes in collagen fibers can be observed in the backward configuration [1], this configuration has become suitable for biomedical imaging.

## 3. Imaging ocular tissues with SHG microscopy

As stated above, the human body is plenty of tissues composed of collagen. These tissues are often the main component of different organs. In particular, the eye is one of them. Although this is not a vital organ (such as the heart or the liver, for instance), it is necessary to have a regular way of living (both humans and animals). Since the middle of nineteenth century, there have been a number of instruments to visualize ocular structures in order to improve the diagnosis and treatment of eye's diseases. Since most ocular elements are transparent, staining procedures are usually required and, under certain experimental conditions, the existing clinical techniques are sometimes not totally appropriate. In that sense, SHG microscopy might be used as a new tool to improve the imaging of some ocular tissues.

The sclera and the cornea are the two structures are the eye's outer tunic, mainly composed of type-I collagen. The former is an opaque connective tissue acting as protective element that gives stability to the ocular globe. Unlike the sclera, the cornea presents high transparency which originates from particular arrangements of the collagen fibers (localized within the stroma, which occupies about 90% of whole corneal thickness). Corneal collagen assembles to form long fibrils with a diameter of approximately 25 nm (in humans) [35]. These are uniformly spaced forming larger bundles or fibers termed “corneal lamellae” (tens of microns in size). In contrast, scleral fibrils have various diameters ranging between 25 and 230 nm [35]. These collagen fibrils also form bundles, however these are not parallel arranged but entangled in individual bundles.

Since type-I collagen is an effective second harmonic generator, both ocular elements can be visualized with SHG imaging microscopy without using labeling techniques. However, the

sclera does not have any contribution to the vision function and this is probably the reason because SHG studies on the sclera are scarce. To our knowledge, Han and colleagues were the first to show SHG images of the sclera [36]. The sclera collagen distribution was analyzed through these images in forward and backward directions. They concluded that the sclera presents inhomogeneous, tube-like structures with thin hard shells, maintaining the high stiffness and elasticity of the tissue. SHG imaging was used by Teng and co-authors to resolve the difference in structural orientations between the collagen fibers of the cornea and the sclera: the corneal collagen is organized in a depth-dependent fashion, whereas the sclera collagen is randomly packed [37]. As an example, **Figure 6** shows SHG images of healthy tissues corresponding to a human cornea and a sclera. A simple visual inspection reveals the evident difference in collagen distribution.

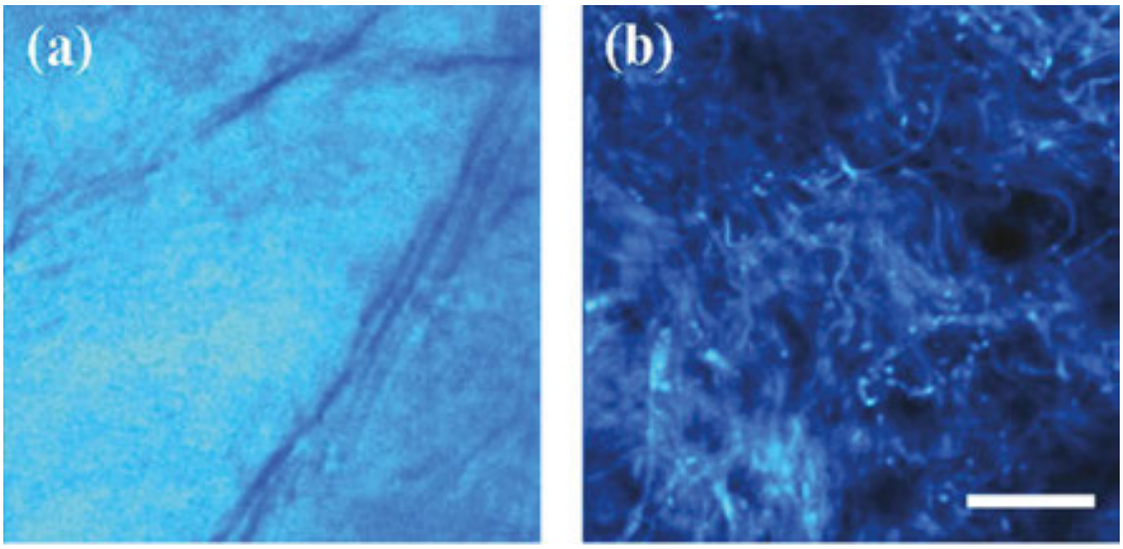


**Figure 6.** Comparison of collagen distributions in SHG images of a human cornea (a) and a piece of human sclera (b). Although the fibers in the sclera present always a non-organized pattern, in the cornea the arrangement depends on a number of factors as explained below. Scale bar: 50 μm.

SHG images of the sclera as a function depth have also been analyzed. At shallow planes collagen bundles were roughly aligned parallel to the limbus. At deeper locations the fibers did not have a specific orientation of alignment [38]. At the posterior pole this arrangement differed. On the external surface undulating thick bundles without a notable major orientation were found. These also had interwoven structures with various orientations. On the internal surface of the sclera fine collagen bundles were observed. These bundles were frequently branched and intermingled. As already mentioned, the sclera has not a direct implication in visual function, however its structures are related to ocular biomechanics and the changes with intraocular pressure or surgery might be interesting in clinical applications.

Unlike the sclera, the cornea has been analyzed with SHG microscopy by many different authors. Since Yeh et al. obtained SHG images in rabbit corneas without exogenous dyes [19] the corneal structure has been studied in a number of animal models (including humans) under several experimental conditions (see for instance [39] and references therein). SHG images of

the cornea have been compared in both forward and backward scattering directions [36]. Although images showed different information, collagen fibers always showed a regular packaging [36, 37]. However, this regular pattern has been shown to change with pathologies [40, 41] or after surgical procedures [42–44]. The corneal stroma also suffers alterations due to scars [45] or changes in the intraocular pressure [46] that have been explored through SHG imaging.

Although SHG microscopy has been used to image the cornea under different experimental conditions, two aspects are really important: (1) the response of the SHG signal to polarized light and (2) the measurement of the stroma organization. Moreover, an objective characterization of structural abnormalities is of great interest to distinguish normal from pathological corneas and the key for possible clinical applications. The next section deals with this topic.

## 4. Measurement of collagen organization in ocular tissues

As previously mentioned, the collagen arrangement could be compromised due to pathological processes, mechanical trauma or denaturation (aging). Due to this, both classification and quantification of collagen arrangement might be a powerful tool in biomedicine as well as in medical diagnosis, in particular for those pathologies associated with collagen disorders occurring at early stages of the disease.

The analysis of the collagen organization has usually been carried out in a qualitative manner. A quantitative analysis would lead to understand changes in corneal stroma caused by intraocular pressure [46], pathological processes [47, 48] or surgery [49] among others. Although there are several techniques to analyze the spatial distribution of collagen, the bidimensional fast Fourier transform (2D-FFT) has often been used for this goal [50].

In particular, the 2D-FFT method has been used with SHG images to compute the degree of organization in corneal collagen in the presence of pathologies [26] or after physical damage

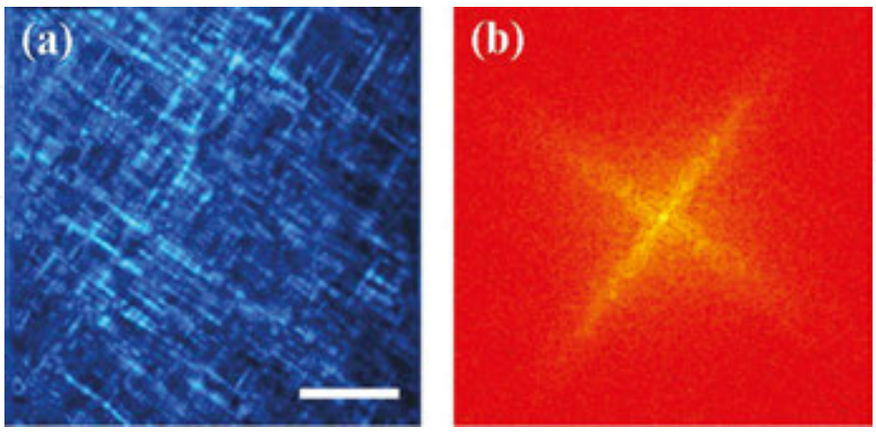


**Figure 7.** (a) SHG images of an eagle cornea with two preferential directions of the collagen fibers (crosshatched pattern) and (b) the associated 2D-FFT image. As expected, the 2D-FFT presents a cross shape as a result of the distribution of the fibers within the imaged corneal layer. Scale bar: 50 μm.

[51]. If the SHG image shows a structure with a preferential orientation, the spatial frequencies of the 2D-FFT spectrum are aligned along the direction orthogonal to that preferential orientation [52]. Nevertheless, the resolution of the 2D-FFT is limited by the noise of the SHG image and an image filtering is often required. The distribution of the spatial frequencies on the 2D-FFT is also generally fitted by an ellipse, and the ratio between its axes is used as a parameter to quantify the collagen organization. However, when a collagen distribution is arranged in a more complex and heterogeneous pattern (interwoven, crosshatched, …), the best fit is a circle and this operation may lead to erroneous conclusions that require a complicate post-processing [53]. **Figure 7** shows a SHG image with a crosshatched appearance of collagen fibers, together with the corresponding 2D-FFT.

In this sense an alternative procedure based on the structure tensor has recently been presented by these authors as a useful tool to classify the spatial distribution of collagen-based tissues through SHG images [54]. The technique has the advantage of differentiate areas with maximum organization from those locations where the orientation of the collagen fibers is not significant. The structure tensor provides relevant parameters such as the spatially-resolved degree of isotropy (DoI) and the histogram of orientation distribution. The former ranges between 0 and 1 and its value increases with the order of the structure (i.e. the more aligned the fibers the higher the DoI). In the latter, it is verified that the narrower the data, the higher the presence of a dominant orientation. Apart from their quantitative information, a visual inspection of both the DoI map and the orientation histogram permits to discriminate between quasi-aligned and non-organized collagen distributions. For a better understanding of this tool, **Figure 8** shows two SHG images with different spatial distributions and the correspond-

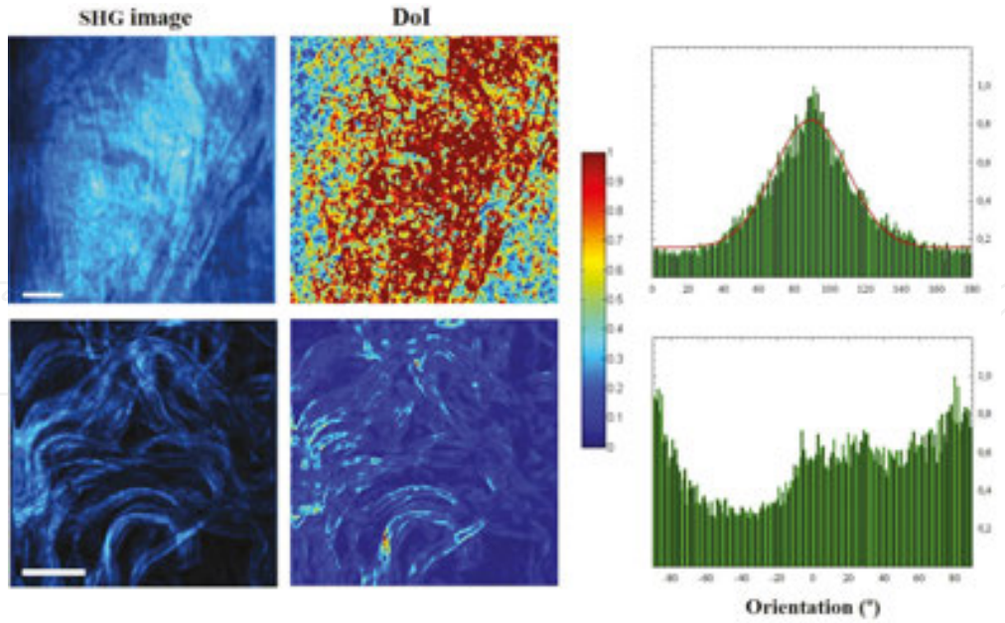


**Figure 8.** SHG images of a human cornea (upper row) and bovine sclera (bottom row) and their respective spatially-resolved DoI and orientation histogram computed through the structure tensor. Detailed information on how these parameters were computed can be found in [54]. Scale bar: 50 μm.

http://dx.doi.org/10.5772/63493

ing structure tensor parameters. At this point, it is important to notice that the combination of SHG microscopy and the structure tensor could help in the diagnosis of abnormal structures and in the tracking of pathologies related to corneal stroma disorders.

## 5. Adaptive optics SHG imaging

Despite optical sectioning capabilities and inherent confocality of SHG microscopy, the imaging of thick samples (3D imaging) is limited by the specimen-induced aberrations. When a femtosecond laser beam is focused into a specimen, the deeper the layer to be imaged, the larger the focal spot size. This leads to a reduction in the effectiveness of the SHG process (i.e. lower SHG signal) and a decrease in the quality of the acquired images, both contrast and resolution (**Figure 9**).

To overpass this, adaptive optics (AO) techniques combining a wavefront sensor and an adaptive device (deformable mirror or spatial light modulator) have been used [55–58]. Most authors have been interested in improving two-photon excitation fluorescence images through AO and experiments dealing with AO-SHG imaging are scarce in the literature [59–62].

Although the ideal situation is to compute and correct for the plane-by-plane aberrations, this is experimentally difficult [63]. In that sense, wavefront sensor-less techniques combined with multiphoton microscopy have been reported [58, 59, 61, 62]. With this approach, at a certain plane within the sample the AO element pre-compensates for the "unknown" aberrations without measuring them, but finding the best image according to a pre-defined image quality metric. Although these are time-consuming procedures due to the use of iterative algorithms such as genetic learning, hill-climbing or stochastic, they have provided significantly improved images with more visible details.

Moreover, the dominant aberration term at deeper layers is the spherical aberration [55, 58, 64]. In order to correct for (or minimize) this unwanted spherical aberration, objective correc-

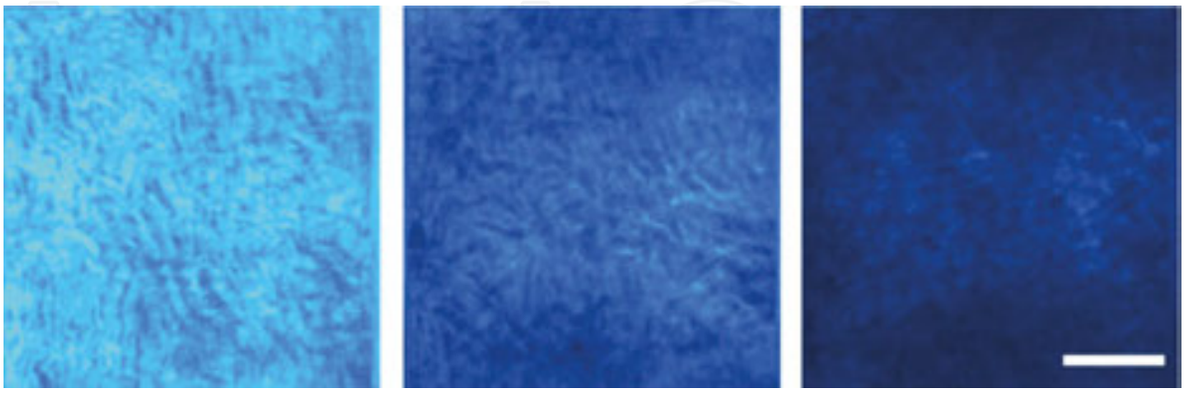

**Figure 9.** SHG images of a rabbit cornea at different depth locations (10, 100 and 100 μm). The reduction in SHG signal is readily visible. This decrease in SHG effectiveness is mainly due to specimen-induced aberrations and scattering. Scale bar: 50 μm.

tion collars [64, 65] and wavefront sensor-less AO devices [55, 58, 62] have been used. The former is a manual method only valid for a defined set of cover thickness values. The latter is faster than usual since only the spherical aberration term has to be corrected. An alternative technique has recently been reported to improve 3D multiphoton imaging [66]. This is based on the manipulation of the spherical aberration pattern of the incident beam while performing fast tomographic SHG imaging. As expected, when inducing spherical aberration the image quality is reduced at best focus, however at deeper planes a better image quality is obtained. This increases the penetration depth and enables improved 3D SHG images even with non-immersion objectives.

Although these AO techniques can be applied to both non-biological and biological samples, there is a special interest when imaging ocular tissues, the cornea in particular. For this ocular structure the features of interest (especially when analyzing pathologies) might be close to the surface or located deep into it. For shallow planes, SHG images are usually of high quality. However when the plane to be imaged is located at a deeper position AO-SHG can be used as a powerful technique to noticeably enhance SHG images corresponding to those deep corneal layers (see **Figure 10** as an example). Those images will have enough contrast and resolution to observe the collagen bundles [66], and any possible abnormal distribution of them across

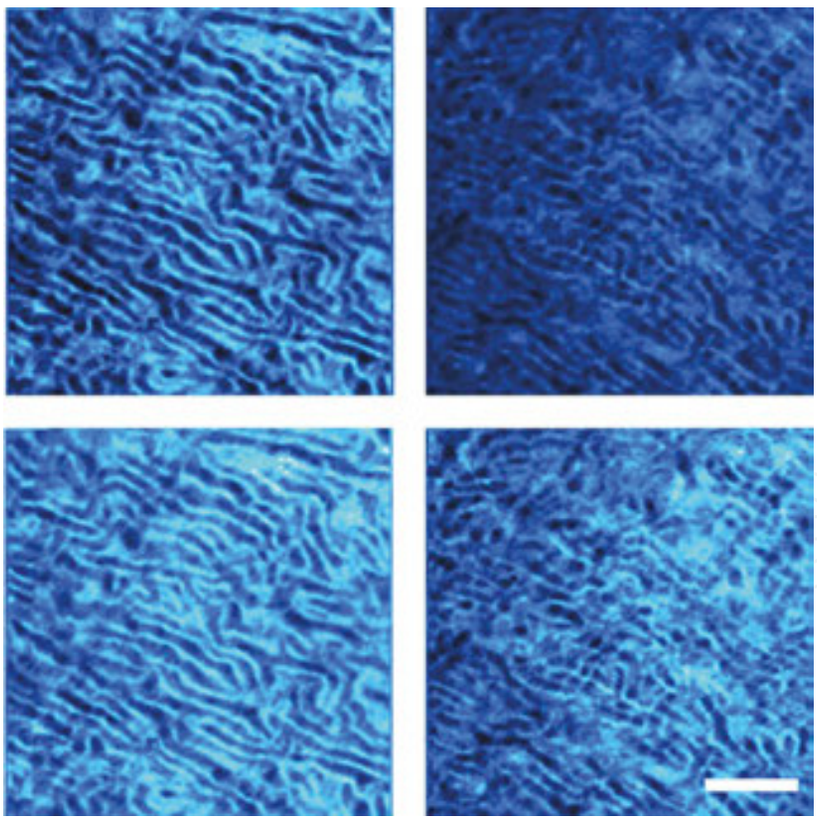

**Figure 10.** Comparison of SHG images before (upper panels) and after (bottom panels) using AO for two different locations within the sample (porcine cornea). It can be observed how AO improves the quality of the images at both locations. However this is more noticeable for deeper locations within the sample. Scale bar: 50 μm.

the imaged area. Future clinical instruments can also benefit from this implementation which leads to a better visualization of the layered ocular structures.

## 6. Polarization-sensitive SHG microscopy

The dependence between polarization and SHG signals in collagen is well recognized [67–69]. The combination of non-linear microscopy and polarization allowed detecting changes in collagen arrangement [70] and has been proposed to characterize collagen-based tissues [71, 72]. Type-I collagen fibers exhibit structural anisotropy that can be characterized by the ratio of hyperpolarizabilities or polarization anisotropy $\varrho = \beta_{xxx}/\beta_{xyy}$, which provides information about the internal collagen structure [33, 73].

The polarization anisotropy depends on the orientation of the collagen triple-helix and the orientation of the induced dipoles along the peptide bonds and the values have been reported to be in the range [-3, 3] [33]. Low values of ϱ are associated with immature collagen [67], aging [69] or loss of arrangement in the collagen distribution [1]. Therefore, polarization-sensitive SHG microscopy provides information about the dipolar distribution within the collagen fibers.

SHG intensity has been reported to vary with the angle between the optical axis of the polarizer and the main orientation of the collagen fibers [33, 69]. Moreover, depending on the spatial distribution of collagen fibers the SHG signal will be differently affected by the incoming polarization state [72, 74, 75] (see **Figure 11** as an example). This fact might be of great importance in SHG imaging not only because the total signal varies (for instance) when changing from linear to circular polarization, but also because more details and extra features might be visible for certain polarization states (see **Figure 12**) [72].

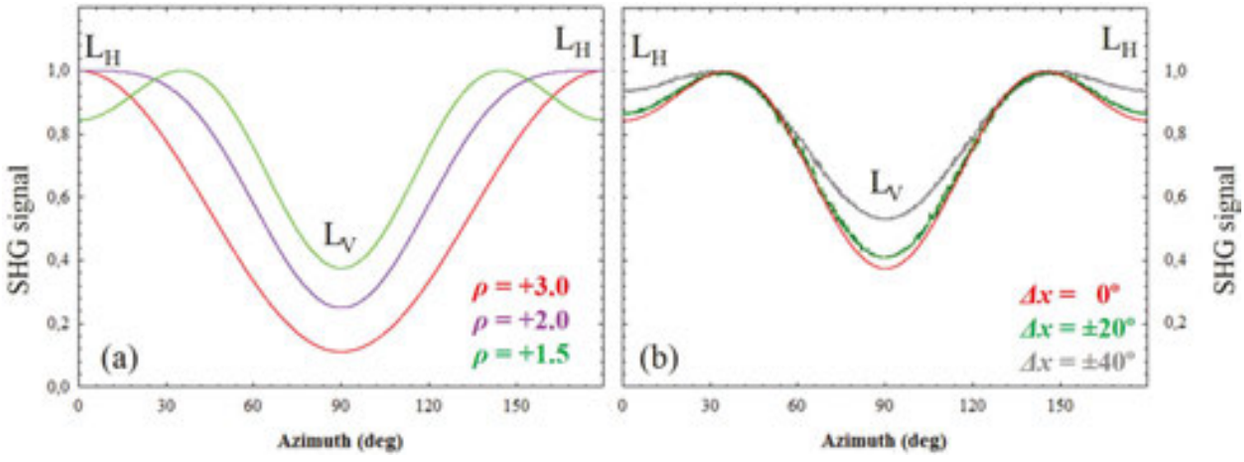


**Figure 11.** SHG intensity as function of the incident linear polarization for three values of ϱ and parallel-arranged collagen fibers (a), and for three different values of structural dispersion, Δx, and ϱ=+1.5 (b). Further details on this can be found in [72].

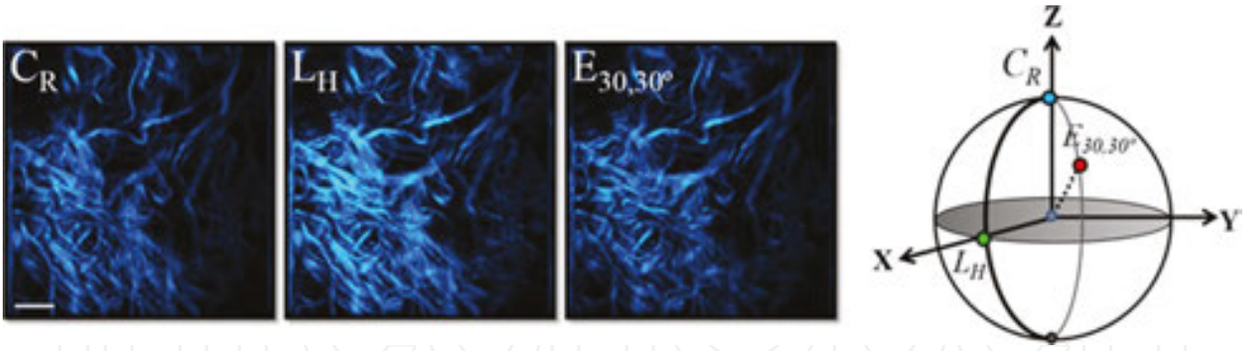


**Figure 12.** SHG images of a bovine sclera recorded for three different incident polarization states. $L_H$, linear horizontal; $C_R$, right circular and $E_{\chi,\psi}$, right elliptical. The location of these polarization states over the Poincaré sphere are shown on the right. Scale bar: 50 μm.

The combination of polarization and SHG signal allows obtaining information about the hierarchical architecture of collagen at molecular scale [76, 77]. This has been used in biopsies to discriminate normal breast from malignant tissue [78], and analyze cancerous ovarian tissues [79].

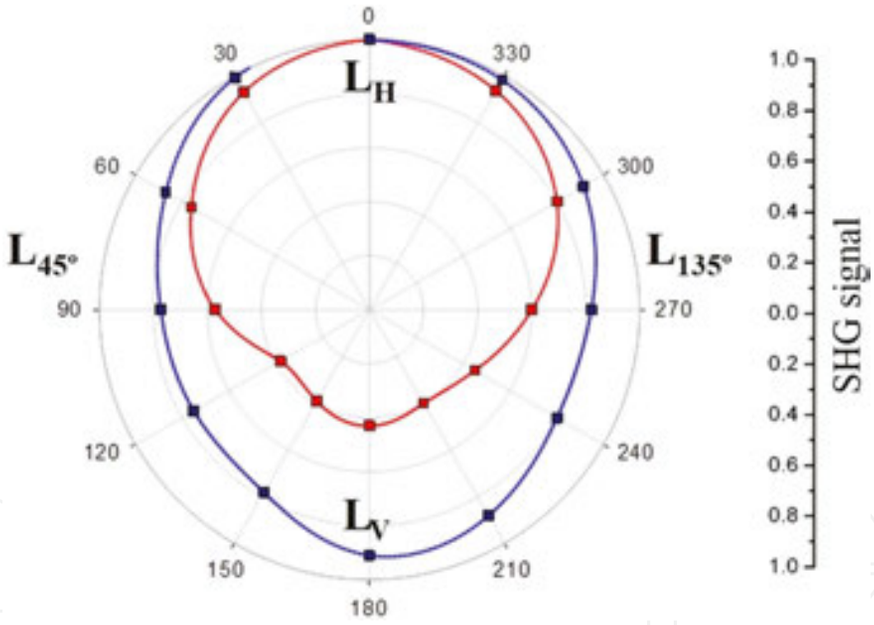


**Figure 13.** Polar diagram representing the normalized SHG intensity distribution as function of incoming polarization of a control (red) and a keratoconus (blue) cornea. The dependence of SHG intensity with incident polarization is stronger in the former probably due to the presence of a dominant direction of the collagen fibers. This does not exist in the latter and the SHG signal hardly depends on the polarization state.

Pathological alterations of the cornea could seriously compromise vision. In this sense polarization-sensitive SHG microscopy has been proved to be effective to detect structural alterations in keratoconus [40]. It has also been employed to analyze the molecular changes produced by high levels of intraocular pressure and to investigate how these modifications produced within the lamellae affect the stroma thickness [80]. As a possible clinical application,

http://dx.doi.org/10.5772/63493

**Figure 13** compares the response to incident linear polarization of a human control and a keratoconus cornea (those presented in **Figure 4**). It can be observed how the SHG signal from the pathological case presents lower dependence with polarization.

## 7. Conclusions

Along this chapter, the principles of SHG processes and the application to biological imaging have been reviewed. SHG microscopy is a non-linear modality with inherent confocality that allows visualizing non-stained tissues composed of collagen and shows features not seen with regular microscopy. SHG intensity depends on both the size and organization of the collagen fibers. Since SHG directionality depends on the distribution of the induced dipoles within the fibers, the registration of the signal in a backscattered direction can be used to observe the collagen architecture within the specimens (**Figure 13**).

In particular, this is a useful tool to image connective ocular tissues such as the sclera and the cornea with high resolution as function of depth. These tissues can be characterized attending the organization of their collagen fibers. Unlike the sclera that usually presents a non-organized distribution, the arrangement of the corneal fibers depends on numerous factors. These collagen organizations have been discussed and a novel method based on the structure tensor to perform quantitative analyses has been proposed. This permits to classify the spatial distribution of the fibers from the SHG images, and can be used for diagnoses of pathologies related to collagen disorders.

However, the efficiency of SHG imaging of thick samples reduces with depth, as the specimen itself induces aberrations and scattering. To overcome this limitation, AO procedures have been implemented into SHG microscopes. The manipulation of the aberration pattern of the incident laser beam has allowed increasing the image quality of SHG images especially at deeper locations.

On the other hand, SHG signal from collagen structures is polarization dependent. This modulation depends on both collagen internal structure (parameter $\varrho$) and the arrangement of the fibers (external organization). The combination of polarization and SHG microscopy has been reported to be effective in detecting structural changes in collagen-related pathological processes. The technique could then be a powerful tool in biomedicine and/or in clinical diagnoses.

## Author details

Juan M. Bueno*, Francisco J. Ávila, and Pablo Artal

*Address all correspondence to: bueno@um.es

Laboratorio de Optica, Universidad de Murcia, Murcia, Spain

## References

[1] R. M. Williams, W. R. Zipfel and W. W. Webb. Interpreting second-harmonic generation images of collagen I fibrils. Biophys. J. 2005; 88(2): 1377–1386.

[2] A. Erikson, J. Ortegren, T. Hompland, C. L. Daviesa and M. Lindgren. Quantification of the second-order non-linear susceptibility of collagen I using a laser scanning microscope. J. Biomed. Opt. 2009; 12(4):044002.

[3] P. N. Butcher and D. Cotter. The elements of nonlinear optics. Cambridge University Press. Cambridge, 1991.

[4] R. W. Boyd. Non-linear optics. Academic Press. San Diego, USA, 1992.

[5] D. A. Kleinman. Theory of second harmonic generation of light. Phys. Rev. 1962; 128(4): 1761–1775.

[6] T. Verbiest, S. Van Elshocht, M. Kauranen, L. Hellemans, J. Snauwaert, C. Nuckolls, T. J. Katz and A. Persoons. Strong enhancement of nonlinear optical properties through supramolecular chirality. Science. 1999; 282(5390):913–915.

[7] L. Moreaux, O. Sandrea and J. Mertz. Membrane imaging by second harmonic generation microscopy. J. Opt. Soc. Am. B. 2000; 17(10):1685–1689.

[8] P. J. Campagnola, A. C. Millard, M. Terasaki, P. E. Hoppe, C. J. Malone and W. Mohler. Three-dimensional high-resolution second-harmonic generation imaging of endogenous structural proteins in biological tissues. Biophys. J. 2002; 82(1):493–508.

[9] S. Fine and W. P. Hansen. Optical second harmonic generation in biological systems. Appl. Opt. 1971; 10(10):2350–2353.

[10] R. Hellwarth and P. Christensen. Nonlinear optical microscopic examination of structure in polycrystalline ZnSc. Opt. Commun. 1974; 12(3):318–322.

[11] J. N. Gannaway and C. J. R. Sheppard. Second harmonic imaging in the scanning optical microscope. Opt. Quantum Electron. 1978; 10(5):435–439.

[12] I. Freund and M. Deutsch. Second harmonic microscopy of biological tissues. Opt. Lett. 1986; 11(2):94–96.

[13] P. J. Campagnola, M. D. Wei, A. Lewis and L. M. Loew. High resolution nonlinear optical microscopy of living cells by second harmonic generation. Biophys. J. 1999; 77(6):3341–3349.

[14] P. J. Campagnola and L. M. Loew. Second-harmonic imaging microscopy for visualizing biomolecular arrays in cells, tissues and organisms. Nat. Biotechnol. 2003; 21(11): 1356–1360.

[15] R. LaComb, O. Nadiarnykh, S. S. Townsend and P. J. Campagnola. Phase matching considerations in second harmonic generation from tissues: effects on emission

directionality, conversion efficiency and observed morphology. Opt. Commun. 2008; 281(7):1823–1832.

[16] S. V. Plotnikov, A. Millard, P. Campagnola and W. Mohler. Characterization of the myosin-based source for second-harmonic generation from muscle sarcomeres. Biophys. J. 2006; 90(2):328–339.

[17] D. A. Dombeck, K. A. Kasischke, H. D. Vishwasrao, M. Ingelsson, B. T. Hyman and W. W. Webb. Uniform polarity microtubule assemblies imaged in native brain tissue by second-harmonic generation microscopy. Proc. Natl. Acad. Sci. U.S.A. 2003; 100(12): 7081–7086.

[18] H. Lodish, A. Berk, C. A. Kaiser, M. Krieger, A. Bretscher, H. Ploegh, A. Amon and M. P. Scott. Molecular cell biology. W.H. Freeman and Company, New York, 2013.

[19] A. T. Yeh, N. Nassif and B. J. Tromberg. Selective corneal imaging using combined second-harmonic generation and two-photon excited fluorescence. Opt. Lett. 2002; 27(23):2082–2084.

[20] G. Cox, E. Kable and M. D. Gorrel. Three-dimensional imaging of collagen using second harmonic generation. J. Struct. Biol. 2003; 141(1):53–62.

[21] S. J. Lin, S. H. Jee and C. Y. Dong. Discrimination of basal cell carcinoma from normal derma stroma by quantitative multiphoton imaging. Opt. Lett. 2006; 31(18):2756–2758.

[22] H. S. Lee, S. W. Teng and C. Y. Dong. Imaging human bone marrow stem cell morphogenesis in polyglycolic acid scaffold by multiphoton microscopy. Tissue Eng. 2006; 12(10):2835–2841.

[23] P. J. Campagnola. Second harmonic generation imaging microscopy: applications to diseases diagnostic. Anal. Chem. 2011; 83(9):3224–3231.

[24] I. Gusachenko, V. Tran, Y. G. Houssen, J. M. Allain and M. C. Schanne-Klein. Polarization-resolved second-harmonic generation in tendon upon mechanical stretching. Opt. Express. 2012; 102(9):2220–2229.

[25] X. Chen, O. Nadiarynkh, S. Plotnikov and P. J. Campagnola. Second harmonic generation microscopy for quantitative analysis of collagen fibrillar structure. Nat. Protoc. 2012; 7(4):654–669.

[26] W. Lo, W. L. Chen, C. M. Hsueh, A. A. Ghazaryan, S. J. Chen, D. H. K. Ma, C. Y. Dong and H. Y. Tan. Fast Fourier transform–based analysis of second-harmonic generation Image in keratoconic cornea. Invest. Opht. Vis. Sci. 2012; 53(7):3501–3507.

[27] H. Yuan-Tan, Y. L. Chang, W. Lo, C. M. Hsueh, W. L. Chen, A. A. Ghazaryan, P. S. Hu, T. H. Young, S. J. Chen and C. Y. Dong. Characterizing the morphologic changes in collagen crosslinked–treated corneas by Fourier transform–second harmonic generation imaging. J. Cat. Refract. Surg. 2013; 39(5):779–788.

[28] R. Seeley, T. Stephens and P. Tate. Anatomy and physiology. McGraw-Hill, Phoenix, 2003.

[29] A. Deniset-Besseau, J. Duboisset, E. Benichou, F. Hache, P. F. Brevet and M. C. Schanne-Klein. Measurement of the second order hyperpolarizability of the collagen triple helix and determination of its physical origin. J. Phys. Chem. B. 2009; 248(4951):73–76.

[30] K. E. Kadler, D. F. Holmes, J. A. Trotter and J. A. Chapman. Collagen fibril formation. Biochem. J. 1996; 316:1–11.

[31] D. A. D. Parry and A. S. Craig. Quantitative electron microscope observations of the collagen fibrils in rat-tail tendon. Biopolymers. 1977; 16(5):1015–1031.

[32] A. Yariv. Quantum electronics. Wiley, New York, 1989.

[33] P. Stoller, P. Celliers, K. Reiser and A. Rubenchik. Quantitative second-harmonic generation microscopy in collagen. Appl. Opt. 2003; 42(25):5209–5219.

[34] I. J. Su, W. L. Chen, Y. F. Chen and C. Y. Dong. Determination of collagen nanostructure from second-order susceptibility tensor analysis. Biophysical J. 2011; 100(8):2053–2062.

[35] Y. Komai and T. Ushiki. The three-dimensional organization of collagen fibrils in the human cornea and sclera. Invest. Ophthalmol. Vis. Sci. 1991; 32(8):2244–2258.

[36] M. Han, G. Giese and J. F. Bille. Second harmonic generation imaging of collagen fibrils in cornea and sclera. Opt. Exp. 2005; 13(15):5791–5797.

[37] S. W. Teng, H. Y. Tan, J. L. Peng, H. H. Lin, K. H. Kim, W. Lo, Y. Sun, W. C. Lin, S. J. Lin, S. H. Jee, P. T. So and C. Y. Dong. Multiphoton autofluorescence and second-harmonic generation imaging of the ex vivo porcine eye. Invest. Ophthalmol. Vis. Sci. 2006; 47(3):1216–1224.

[38] M. Yamanari, S. Nagase, S. Fukuda, K. Ishii, R. Tanaka, T. Yasui, T. Oshika, M. Miura and Y. Yasuno. Scleral birefringence as measured by polarization-sensitive optical coherence tomography and ocular biometric parameters of human eyes in vivo. Biomed. Opt. Express. 2014;5(5):1391–1402.

[39] J. M. Bueno, E. J. Gualda and P. Artal. Analysis of corneal stroma organization with wavefront optimized nonlinear microscopy. Cornea. 2011; 30(6):692–701.

[40] H. Y. Tan, Y. Sun, W. Lo, S. J. Lin, C. H. Hsiao, Y. F. Chen, S. C. Huang, W. C. Lin, S. H. Jee, H. S. Yu and C. Y. Dong. Multiphoton fluorescence and second harmonic generation imaging of the structural alterations in keratoconus ex vivo. Invest. Ophthalmol. Vis. Sci. 2006; 47(12):5251–5259.

[41] C. M. Hsueh, W. Lo, W. L. Chen, V. A. Hovhannisyan, G. Y. Liu, S. S. Wang, H. Y. Tan and C. Y. Dong. Structural characterization of edematous corneas by forward and backward second harmonic generation imaging. Biophys. J. 2009; 97(4):1198–1205.

[42] T.-J. Wang, W. Lo, C. M. Hsueh, M. S. Hsieh, C. Y. Dong and F. R. Hu. Ex vivo multiphoton analysis of rabbit corneal wound healing following conductive keratoplasty. J. Biomed. Opt. 2008; 13(3):034019.

[43] E. J. Gualda, J. R. Vázquez de Aldana, M. C. Martínez-García, P. Moreno, J. Hernández-Toro, L. Roso, P. Artal and J. M. Bueno. Femtosecond infrared intrastromal ablation and backscattering-mode adaptive-optics multiphoton microscopy in chicken corneas. Biomed. Opt. Express. 2011; 2(11):2950–2960.

[44] J. M. Bueno, E. J. Gualda, A. Giakoumaki, P. Pérez-Merino, S. Marcos and P. Artal. Multiphoton microscopy of ex-vivo corneas after collagen cross-linking. Invest. Ophthalmol. Vis. Sci. 2011; 52(8):5325–5331.

[45] S. W. Teng, H. Y. Tan, Y. Sun, S. J. Lin, W. Lo, C. M. Hsueh, C. H. Hsiao, W. C. Lin, S. C. Huang and C. Y. Dong. Multiphoton fluorescence and second-harmonic-generation microscopy for imaging structural alterations in corneal scar tissue in penetrating full-thickness wound. Arch. Ophthalmol. 2007; 125(7):977–978.

[46] Q. Wu and A. T. Yeh. Rabbit cornea microstructure response to changes in intraocular pressure visualized by using nonlinear optical microscopy. Cornea. 2008; 27(2):202–208.

[47] N. Morishige, A. J. Wahlert, M. C. Kenney, D. J. Brown, K. Kawamoto, T. Chikama, T. Nishida and J. V. Jester. Second-harmonic imaging microscopy of normal human and keratoconus cornea. Invest. Ophthalmol. Vis. Sci. 2007; 48(3):1087–1094.

[48] N. Morishige, N. Yamada, X. Zhang, Y. Morita, N. Yamada, K. Kimura, A. Takahara and K. H. Sonoda. Abnormalities of stromal structure in the bullous keratopathy cornea identified by second harmonic generation imaging microscopy. Invest. Ophthalmol. Vis. Sci. 2012; 53(8):4998–5003.

[49] K. Plamann, F. Aptel, C. L. Arnold, A. Courjaud, C. Crotti, F. Deloison, F. Druon, P. Georges, M. Hanna, J. M. Legeais, F. Morin, É. Mottay, V. Nuzzo, D. A. Peyrot and M. Savoldelli. Ultrashort pulse laser surgery of the cornea and the sclera. J. Opt. 2010; 12(8): 084002.

[50] H. G. Adelman. Butterworth equations for homomorphic filtering of images. Comp. Biol. Med. 1998; 28(2):169–181.

[51] P. Matteini, F. Ratto, F. Rossi, R. Cicchi, C. Stringari, D. Kapsokalyvas, F. S. Pavone and R. Pini. Photothermally-induced disordered patterns of corneal collagen revealed by SHG imaging. Opt. Express. 2009; 17(6):4868–4878.

[52] J. C. Russ. The image processing handbook. CRC Press, Boca Raton, 2007.

[53] J. M. Bueno, R. Palacios, M. K. Chessey and H. Ginis. Analysis of spatial lamellar distribution from adaptive-optics second harmonic generation corneal images. Biom. Opt. Express. 2013; 4(7):1006–1013.

[54] F. J. Avila and J. M. Bueno. Analysis and quantification of collagen organization with the structure tensor in second harmonic microscopy images of ocular tissues. Appl. Opt. 2015; 54(33):9848–9854.

[55] L. Sherman, J. Y. Ye, O. Albert and T. B. Norris. Adaptive correction of depth-induced aberrations in multiphoton scanning microscopy using a deformable mirror. J. Microsc. 2002; 206:65–71.

[56] P. Marsh, D. Burns and J. Girkin. Practical implementation of adaptive optics in multiphoton microscopy. Opt. Express. 2003; 11(10):1123–1130.

[57] M. Rueckel, J. A. Mack-Bucher and W. Denk. Adaptive wavefront correction in two-photon microscopy using coherence-gated wavefront sensing. P. Natl. Acad. Sci. U. S. A. 2006; 103(46):17137–17142.

[58] D. Debarre, E. J. Botcherby, T. Watanabe, S. Srinivas, M. J. Booth and T. Wilson. Image-based adaptive optics for two-photon microscopy. Opt. Lett. 2009; 34(16):2495–2497.

[59] A. Jesacher, A. Thayil, K. Grieve, D. Debarre, T. Watanabe and T. Wilson. Adaptive harmonic generation microscopy of mammalian embryos. Opt. Lett. 2009; 34(20):3154–3156.

[60] J. M. Bueno, E. J. Gualda and P. Artal. Adaptive optics multiphoton microscopy to study ex vivo ocular tissues. J. Biomed. Opt. 2010; 15(6):066004.

[61] J. Antonello, T. van Werkhoven, M. Verhaegen, H. H. Truong, C. U. Keller and H. C. Gerritsen. Optimization-based wavefront sensorless adaptive optics for multiphoton microscopy. J. Opt. Soc. Am. A. 2014; 31(6):1337–1347.

[62] M. Skorsetz, P. Artal and J. M. Bueno. Performance evaluation of a sensorless adaptive optics multiphoton microscope. J. Microscopy. 2015; doi: 10.1111/jmi.12325.

[63] M. Skorsetz, P. Artal and J. M. Bueno. Performance evaluation of a sensorless adaptive optics multiphoton microscope. J. Micros. 2015; 261(3):246–258

[64] W. Lo, Y. Sun, S. J. Lin, S. H. Jee and C. Y. Dong. Spherical aberration correction in multiphoton fluorescence imaging using objective. J. Biomed. Opt. 2005; 10(3):034006.

[65] P. A. Muriello and K. W. Dunn. Improving signal levels in intravital multiphoton microscopy using an objective correction collar. Opt. Commun. 2008; 281(7):1806–1812.

[66] J. M. Bueno. Adaptive optics multiphoton microscopy: probing the eye more deeply. Opt. Photo. News. 2014; 25(1):48–55.

[67] S. Roth and I. Freund. Second harmonic generation in collagen. J. Chem. Phys. 1979; 70(4):1637–1643.

[68] S. Roth and I. Freund. Optical second-harmonic scattering in rat-tail tendon. Biopolymers. 1981; 20(6):1271–1290.

[69] I. Freund, M. Deutsch and A. Sprecher. Connective tissue polarity: optical second-harmonic microscopy, crossed-beam summation, and small-angle scattering in rat-tail tendon. Biophys. J. 1986; 50(4):693–712.

[70] P. Stoller, K. M. Reiser, P. M. Celliers and A. M. Rubenchik. Polarization-modulated second harmonic generation in collagen. Biophys. J. 2002; 82(6):3330–3342.

[71] C. H. Lien, K. Tilbury, S. J. Chen and P. J. Campagnola. Precise, motion-free polarization control in second harmonic generation microscopy using a liquid crystal modulator in the infinity space. Biom. Opt. Express. 2013; 4(10):1991–2002.

[72] F. J. Ávila, O. Barco and J. M. Bueno. Polarization dependence of collagen-aligned tissues imaged with second harmonic generation microscopy. J. Biom. Opt. 2015; 20(8): 086001.

[73] I. Gusachenko, G. Latour and M. C. Schanne-Klein. Polarization-resolved Second Harmonic microscopy in anisotropic thick tissues. Opt. Express. 2010; 18(18):19339–19352.

[74] O. Nadiarnykh and P. J. Campagnola. Retention of polarization signatures in SHG microscopy of scattering tissues through optical clearing. Opt. Express. 2009; 17(7): 5794–5806.

[75] O. del Barco and J. M. Bueno. Second harmonic generation signal in collagen fibers: role of polarization, numerical aperture, and wavelength. J. Biom. Opt. 2012; 17(4): 045005.

[76] F. Tiaho, G. Recher and D. Rouède. Estimation of helical angles of myosin and collagen by second harmonic. Opt. Express. 2007; 15(19):12286–12295.

[77] W. L. Chen, T. H. Li, P. J. Su, C. K. Chou, P. T. Fwu, S. J. Lin, D. Kim, P. T. C. So and C. Y. Dong. Second-order susceptibility imaging with polarization-resolved, second harmonic generation microscopy. Proc. SPIE. 2010; 7569(75691):1–7.

[78] R. Ambekar, T. Y. Lau, M. Walsh, R. Bhargava and K. C. Toussaint. Quantifying collagen structure in breast biopsies using second-harmonic generation imaging. Biom. Opt. Express. 2012; 3(9):2021–2035.

[79] K. Tilbury and P. J. Campagnola. Applications of second-harmonic generation imaging microscopy in ovarian and breast cancer. Perspect. Medicin. Chem. 2015; 16(7):21–32.

[80] A. Benoit, G. Latour, S. K. Marie-Claire and J. M. Allain. Simultaneous microstructural and mechanical characterization of human corneas at increasing pressure. J. Mech. Behav. Biomed. Mater. 2015; 60:93–105.

IntechOpen